Inorganic Chemistry

Article

pubs.acs.org/IC

Successive Heterolytic Cleavages of H_2 Achieve N_2 Splitting on Silica-Supported Tantalum Hydrides: A DFT Proposed Mechanism

Xavier Solans-Monfort,*[,†] Catherine Chow,[‡,∥] Eric Gouré,[‡,⊥] Yasemin Kaya,[‡] Jean-Marie Basset,*[,‡,#] Mostafa Taoufik,[‡] Elsje Alessandra Quadrelli,*[,‡] and Odile Eisenstein*[,§]

[†]Departament de Química, Universitat Autònoma de Barcelona, 08193 Bellaterra, Spain

[‡]Université de Lyon, Institut de Chimie de Lyon, C2P2 (CNRS, CPE Lyon, Université Lyon 1) Ecole Supérieure de Chimie Physique Electronique de Lyon, 43 Boulevard du 11 Novembre 1918, F-69616 Villeurbanne Cedex, France

[§]Institut Charles Gerhardt, UMR 5253 CNRS, Université Montpellier 2, cc 1501, Place E. Bataillon, F-34095 Montpellier, France

Supporting Information

ABSTRACT: DFT(B3PW91) calculations have been carried out to propose a pathway for the N_2 cleavage by H_2 in the presence of silica-supported tantalum hydride complexes $[(\equiv SiO)_2TaH_x]$ that forms $[(\equiv SiO)_2Ta(NH)(NH_2)]$ (*Science* **2007**, *317*, 1056). The calculations, performed on the cluster models $\{\mu\text{-}O[(HO)_2SiO]_2\}TaH_1$ and $\{\mu\text{-}O[(HO)_2SiO]_2\}TaH_3$, labelled as $(\equiv SiO)_2TaH_x$ (x = 1, 3), show that the direct hydride transfers to coordinated N-based ligands in $(\equiv SiO)_2TaH(\eta^2\text{-}N_2)$ and $(\equiv SiO)_2TaH(\eta^2\text{-}HNNH)$ have high energy barrier barriers. These high energy barriers are due in part to a lack of energetically accessible empty orbitals in the negatively charged N-based ligands. It is shown that a succession of proton transfers and reduction steps (hydride transfer or 2 electron reduction by way of dihydride reductive coupling) to the nitrogen-based ligands leads to more energetically accessible pathways. These proton transfers, which occur by way of heterolytic activation of H_2, increase the electrophilicity of the resulting ligand (diazenido, N_2H^-, and hydrazido, $NHNH_2^-$, respectively) that can thus accept a hydride with a moderate energy barrier. In the case of $(\equiv SiO)_2TaH(\eta^2\text{-}HNNH)$, the H_2 molecule that is adding across the Ta−N bond is released after the hydride transfer step by heterolytic elimination from $(\equiv SiO)_2TaH(NH_2)_2$, suggesting that dihydrogen has a key role in assisting the final steps of the reaction without itself being consumed in the process. This partly accounts for the experimental observation that the addition of H_2 is needed to convert an intermediate, identified as a diazenido complex $[(\equiv SiO)_2TaH(\eta^2\text{-}HNNH)]$ from its ν(N−H) stretching frequency of 3400 cm^{-1}, to the final product. Throughout the proposed mechanism, the tantalum remains in its preferred high oxidation state and avoids redox-type reactions, which are more energetically demanding.

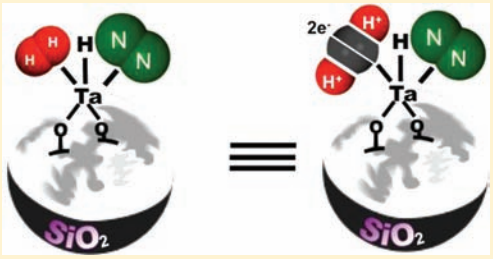

INTRODUCTION

Dinitrogen cleavage has long been recognized as an obligatory step for the entry of this abundant yet stable and relatively inert feedstock into the cycle of man-made and biological nitrogen-containing chemicals.[1,2] While the triple bond between the two nitrogen atoms renders this molecule very stable, as indicated by its large bond dissociation energy of 225 kcal mol^{-1}, thermodynamics show that its transformation into chemicals such as ammonia is possible (ΔH° = −11.1 kcal mol^{-1}, ΔS° = −23.7 kcal mol^{-1} K^{-1}).[2] The obstacle to N_2 transformation essentially lies in its inertness, due to multiple factors such as its apolarity, a large HOMO−LUMO gap of 22.9 eV, a negative electron affinity, and a high ionization energy of 15.58 eV. That is why catalysis plays a major role in dinitrogen transformation to the thermodynamically allowed production of ammonia from N_2. The transformation of N_2 to ammonia is currently achieved at ambient temperature and atmospheric pressure in biological systems via the nitrogenase enzymes.[3] Alternatively, in non-biological chemistry, the reduction of N_2 to ammonia under mild conditions is a major challenge. The Haber-Bosch process, which is used to synthesize 150 million tons of ammonia per year, requires temperatures around 450 °C and pressures of between 200 and 300 atm.[4]

The literature on N_2 reduction to NH_3 is abundant in heterogeneous, homogeneous, and biomimetic catalysis. The heterogeneous Haber-Bosch system has been intensively studied. One of the particular aspects of this surface chemistry is the demonstration of the elementary steps and kinetics of the reduction of N_2 by H_2 to give ammonia. In particular the dissociation of dinitrogen is assumed to occur on defect sites of the metallic surface (typically iron) leading to surface nitrides in which each nitrogen atom is linked to three surface metal atoms. The activation of dihydrogen does not constitute a problem since it can be activated at a much lower temperature and can move easily on the surface of the metallic particle.[5,6] In molecular and biomimetic chemistry,[7] the discovery of the first dinitrogen complex by Allen and Senoff in 1965[8] gave clues to the possible role of the metal in the nitrogenase system. The principles involved in the reduction of N_2 were established by the groups of

Received: March 6, 2012
Published: June 19, 2012

   dx.doi.org/10.1021/ic300498b | *Inorg. Chem.* 2012, 51, 7237−7249

Chatt,[9] Hidai,[10,11] and Shilov.[12] In 2003, Schrock and Yandulov showed how N_2 could be converted catalytically to NH_3 in the presence of $Mo[(HIPTN)_3N]$ (HIPTN = {3,5-(2,4,6-*i*-$Pr_3C_6H_2)_2C_6H_3$}NCH_2CH_2) using consecutive addition of protons from a lutidinium salt and electrons from hexamethyldecachromocene.[13] More recently, catalytic conversion of dinitrogen into ammonia under very mild conditions was achieved also using a dinuclear molybdenum dinitrogen precursor, $CoCp_2$ as an electron donor, and lutidinium salt as a proton donor.[14]

Noncatalytic conversion of N_2 to ammonia has been achieved using various methods to provide a source of electrons. Electrochemical[15] or photochemical processes[16] have been used as sources of energy to achieve the $N_2 + H_2$ to NH_3 conversion. Very recently, N_2 reduction and hydrogenation to ammonia by a molecular iron−potassium complex was achieved.[17] Many research groups have focused their attention on the N_2 splitting and/or functionalization. In this way, bare metals under matrix-isolation conditions have been found to cleave N_2.[18] In addition, a larger palette of experimental conditions has been used to cleave the dinitrogen bond in either di- or polymetallic complexes of N_2 even though ammonia is not produced or is not the sole product of reaction.[19−21] Molecular dihydrogen is rarely used as the reducing agent in molecular complexes.[21,22] On the other hand, the functionalization of dinitrogen has also been achieved in several cases with silane, borane, and CO usually via the coordination of N_2 to a dinuclear complex.[22,23]

We are interested, in this article, in the unique example offered by surface chemistry that achieves stoichiometric reaction of N_2 and H_2 with silica-supported tantalum hydride complexes $[(\equiv SiO)_2TaH]$ and $[(\equiv SiO)_2TaH_3]$ forming the silica-supported amido−imido complex $[(\equiv SiO)_2Ta(NH)(NH_2)]$ as shown by us and co-workers.[24] The reaction takes place at 250 °C and low pressures of H_2 and N_2 without the need for an additional reagent. The singularity of this process is that tantalum hydrides act as monometallic species capable of splitting N_2 with molecular dihydrogen as the reducing agent.

In parallel to the experiments, a large number of theoretical studies have been carried out on the most relevant systems mentioned above. Several of them have centered their efforts on understanding the reaction pathways leading to the formation of NH_3. The heterogeneous catalytic cleavage of N_2 has been studied by several authors.[6,25] According to their DFT calculations, N_2 cleavage is usually the key step, and it most likely occurs at step sites of the surface. The molybdenum complexes studied by Schrock and Yandulov have likewise attracted considerable attention. Calculations using small and larger models of the real systems reproduce reasonably well the experimental results.[26] The processes involving N_2 activation and cleavage by polymetallic species without forming NH_3 have also attracted the attention of theoretical chemists.[27] In these cases, unlike the two previous systems, the activation of the N_2 ligand is usually accomplished when N_2 is side-on coordinated and/or bridged between two metal centers. Likewise, the hydrogenation of various nitrogen metal complexes such as the nitrido derivative has been considered.[27q] Finally, the reactivity of silica-supported tantalum hydrides with N_2 and H_2 has been studied through DFT calculations.[28] The authors proposed a mechanism consisting of three successive hydride transfers, usually with high energy barriers, which is compatible with the high temperature used in the experiments.

In this article, we wish to focus on the mechanistic issues for the stoichiometric N_2 splitting by silica-supported tantalum hydrides. We have explored pathways that have not been considered in the previous study.[28] This leads us to propose a route that is different from those previously suggested. The new pathway is characterized by minimizing the number of steps where the oxidation state of the tantalum is modified, which can be energy demanding. This is possible by making use of the ability of H_2 to split in a heterolytic manner and to provide a proton to be transferred to nitrogen and a hydride as a reducing agent.[29,30] The pathway proposed in this article also fits better with the nature of intermediates suggested by experiments.[24]

MODELS, COMPUTATIONAL DETAILS, AND EXPERIMENTAL SECTION

Model. The grafted complex is modeled using a molecular approach with the cluster shown in Figure 1. The surface oxygen atoms covalently

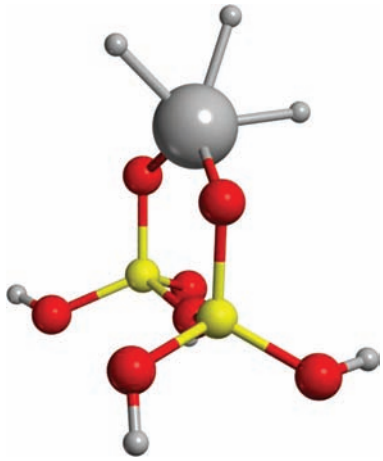

Figure 1. Cluster model for the silica supported tantalum trihydride.

bonded to the tantalum center have been assumed to be vicinal and the surface is represented by including the first SiO_4 shell. This model is similar to most of those used previously for representing silica-supported transition metal hydrides[31] and supported Schrock-type olefin metathesis catalysts.[32,33] This model has been shown to correctly reproduce the spectroscopic properties of $[(\equiv SiO)_2Ta(NH)(NH_2)]$ and its reactivity with H_2 and NH_3.[24,34,35] It is noteworthy that this molecular approach gives results that are similar to those obtained with calculations using periodic boundaries conditions.[24,33,34]

Computational Details. Calculations have been carried out with the B3PW91[36,37] density functional and the Gaussian 03 package.[38] Silicon and tantalum atoms have been represented with the quasi-relativistic effective core pseudopotentials (RECP) of the Stuttgart−Bonn group and the associated basis sets augmented with a polarization function.[39] All other atoms (O, N, and H) have been represented by the Dunning's correlation consistent aug-cc-pVDZ basis sets.[40] All optimizations were performed without any geometry constraint and the nature of the extrema was checked by analytical calculations of the frequencies. Calculations were also carried out with the M06 functional[41] giving results similar to those obtained with the B3PW91. For consistency with previous published work on silica supported complexes relevant to either activation of N_2 and NH_3[24,34,35] or to olefin metathesis catalysts,[32,33] we present the results with B3PW91. This choice allows also a more relevant comparison with the work of Li and Li on the same reaction.[28] The results with the M06 functional (energies and coordinates) are presented in the Supporting Information. The values and the natures of the vectors associated with the imaginary frequencies are given in the Supporting Information. The Intrinsic Reaction Coordinate (IRC) was calculated to ensure the nature of the two minima interconnected through the transition states.

dx.doi.org/10.1021/ic300498b | Inorg. Chem. 2012, 51, 7237−7249

Scheme 1. Energies and Gibbs Energies at 298 and 523 K (in Parentheses), in kcal mol^{-1}, of Minima and Transition States for the Set of Reactions between 1III or 1V and N_2[a]

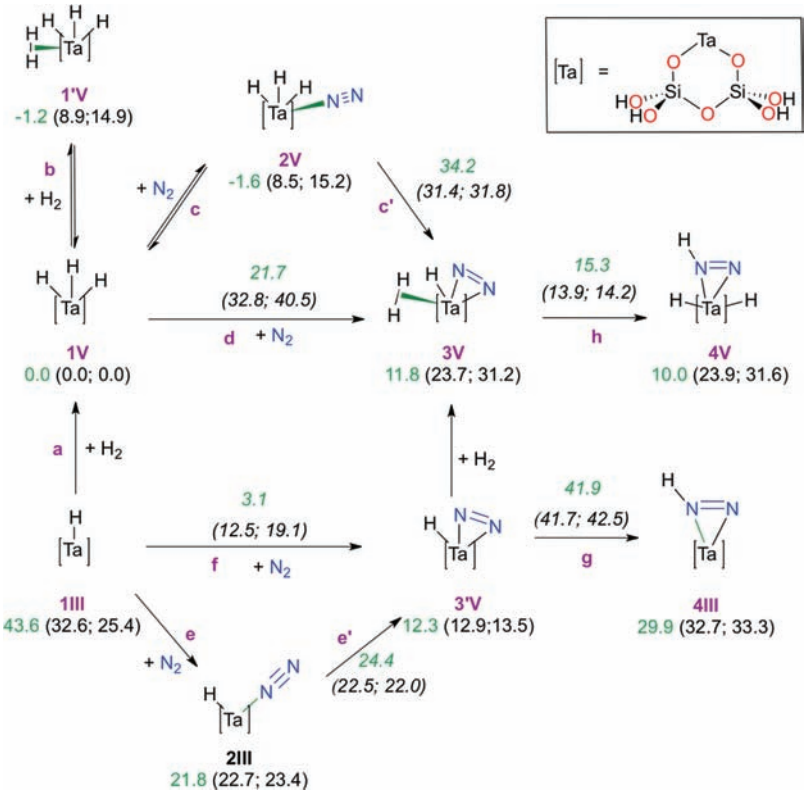

[a]The origin of energies is separated **1V**, H_2, and N_2. A green line between a ligand and tantalum represents a ligand-to-metal donor−acceptor bond. The energies and Gibbs energies next to the arrows given in italics are those for the transition state relative the reactant at the start of the arrow. The geometries of all extrema are shown in Figure 2.

The reported IR frequencies were calculated within the harmonic approximation and were not scaled. Three sets of energies are used to discuss the obtained results: (i) electronic energies E without ZPE corrections, (ii) Gibbs energies (G_{523K}) computed with Gaussian 03 at 1 atm and 523.15 K (highest experimental temperature used), and (iii) Gibbs energies (G_{298K}) at 1 atm and 298.15 K. Gibbs energies are computed assuming an ideal gas, unscaled harmonic vibrational frequencies, and the rigid rotor approximation. This is an approximate way of evaluating the entropic contributions, but no simple procedure applicable to the experimental conditions is available. Great caution should be exerted when considering the calculated values of the entropic contribution in a reaction in which gases are put into contact with a solid. While the absolute entropic contributions are difficult to determine, comparing reactions, which have similar changes in molecularity, presents fewer difficulties. Neglecting totally the entropic contributions by using the energies in place of the Gibbs energies would introduce larger biases in the results.

The d^2 tantalum complexes may have an accessible open shell triplet state. Calculations with the B3PW91 functional show that the triplet state is lower than the closed shell singlet for the tantalum monohydride (**1III** in the following) and the end-on N_2 coordinated adduct (**2III** in the following) by 6.8 kcal mol^{-1} and 3.4 kcal mol^{-1}, respectively. Thus, the essential of the reaction pathways occurs on the singlet state potential energy surface. The consideration of the triplet state for **1III** and **2III** will not modify the overall description of the pathway. Consequently, the triplet state for these two species will not be considered further.

Additional Experiments for the Reaction of N_2 with [(≡SiO)$_2$TaH$_x$]. The following experiments were carried out in continuation of our previous results.[24] Two self-supporting pellets containing the silica-supported mixture of tantalum hydrides [(≡SiO)$_2$TaH$_x$] were prepared as previously described.[24] Prior to dinitrogen addition, the pellets were heated at 150 °C under a dynamic vacuum for 3 h in order to increase the amount of [(≡SiO)$_2$TaH] with respect to of [(≡SiO)$_2$TaH$_3$].[42] The first pellet was exposed to a dinitrogen atmosphere (500 Torr) and analyzed by in situ IR as previously.[24] The expected dinitrogen adduct, characterized by $\nu(N_2) = 2280$ cm^{-1}, was observed. After treatment under a vacuum, which led to the disappearance of the $\nu(N_2)$ band, the solid was analyzed by elemental analysis (wt %: Ta = 11.4; N = 0.94). The second pellet was exposed to N_2, heated at 250 °C, and analyzed by IR (Figure S1). A lower concentration of intermediate species characterized by $\nu(N_2H_x) = 3400$ cm^{-1} was observed for this monohydride-enriched sample than with the regular sample of tantalum hydride mixture.[24] Only traces of the imido amido Ta$^{(V)}$ final product assigned to reacted tantalum hydrides were observed. No dihydrogen was detected in the gas phase.

RESULTS

A detailed exploration of the potential energy surface of the N_2 splitting by {μ-O[(HO)$_2$SiO]$_2$}TaH$_x$ (shown in Figure 1 for $x = 3$), represented as (≡SiO)$_2$TaH$_x$ hereafter, was carried out using the mono- ($x = 1$) and trihydride ($x = 3$) complexes as reactive species. The energies, E, and Gibbs energies, G, at 298 and 523.15 K of the reaction profiles are presented in Schemes 1−3. Figures 2−4 show the optimized structures of all extrema, and Figure 5 summarizes the global energy profiles using G_{523K} values.

Initial (≡SiO)$_2$TaH$_x$ Hydrides. The results are shown in Scheme 1 and Figure 2. Hydrogenolysis of the d^0 silica-grafted organometallic tantalum complex (≡SiO)$_2$Ta{=CH(t-Bu)}-{(−CH$_2$(t-Bu)} yields a mixture of hydrides, (≡SiO)$_2$TaH$_x$,

dx.doi.org/10.1021/ic300498b | Inorg. Chem. 2012, 51, 7237−7249

Scheme 2. Energies and Gibbs Energies at 298 and 523 K (in Parentheses), in kcal mol^{-1}, of Minima and Transition States for the Reactions Initiated by 3V[a]

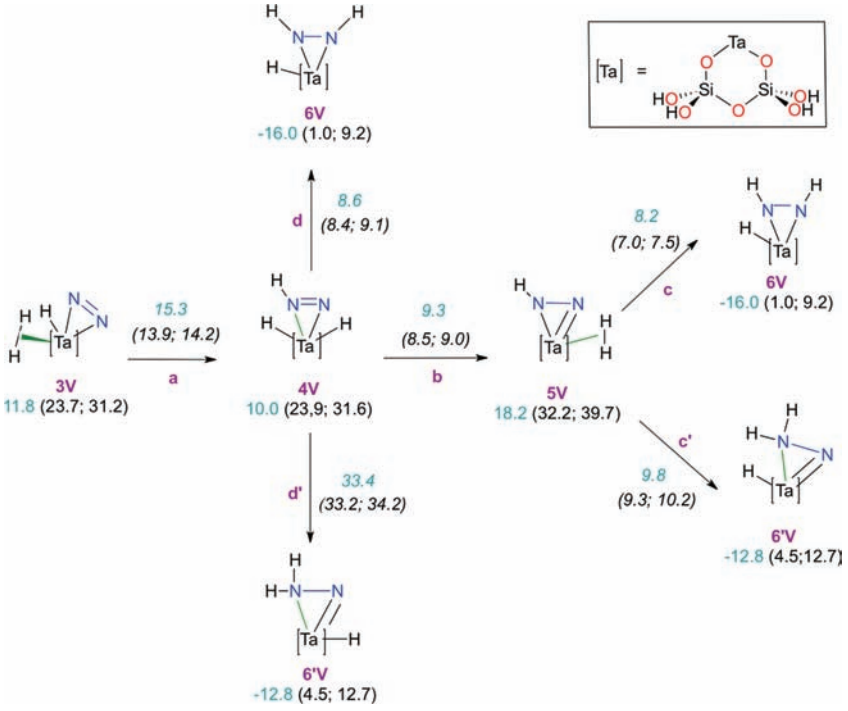

[a]The origin of energies is separated **1V**, H_2 and N_2. A green line between ligand and tantalum represents a ligand-to-metal donor−acceptor bond. The energies and Gibbs energies next to the arrows given in italic are those for the transition state relative the reactant at the start of the arrow. The geometries of all extrema are shown in Figure 3.

the two major ones being attributed to a monohydride, $(\equiv SiO)_2Ta^{(III)}H$, and a trishydride, $(\equiv SiO)_2Ta^{(V)}H_3$, modeled in this study by **1III** and **1V**, respectively.[42] The monohydride $(\equiv SiO)_2TaH$, **1III**, which has a formal d^2 tantalum center, has a trigonal planar geometry at the metal center with standard Ta−H and Ta−O bond distances. The $(\equiv SiO)_2TaH_3$ structure **1V** is related to that of Cp_2TaH_3 since the three Ta−H bonds are in the plane that bisects the O−Ta−O angle as they do in the $cyclopentadienyl_{centroid}$−Ta−$cyclopentadienyl_{centroid}$.[43] In this trihydride, **1V**, the average distance between two cis hydrogens is 1.871 Å, which indicates an absence of interaction between them.

The reaction **1III** + H_2 → **1V** (**a** in Scheme 1) is highly exothermic (ΔE = −43.6 kcal mol^{-1}), and although the entropic contribution is unfavorable, **1V** has a significantly lower Gibbs energy than the separated **1III** and H_2 in the temperature range used in the experimental setting (ΔG_{298K} = −32.6 kcal mol^{-1}, ΔG_{523K} = −25.4 kcal mol^{-1}). The energy of **1V** and free H_2 and N_2 is used in the following as reference.

Formation of the Side-on N_2 Complexes $(\equiv SiO)_2TaH_x(\eta^2\text{-}N_2)$. The very small coordination energy of N_2 to **1V** (**c** in Scheme 1) of ΔE = −1.6 kcal mol^{-1} (−5.6 kcal mol^{-1} with M06) makes N_2 coordination disfavored by the entropic contribution. Using the standard procedure described in the Computational Details, the Gibbs energies of $(\equiv SiO)_2TaH_3(\eta^1\text{-}N_2)$, **2V**, are 8.5 kcal mol^{-1} at 298 K and 15.2 kcal mol^{-1} at 523 K. In **2V**, N_2 is end-on coordinated with a long Ta−N bond distance of 2.446 Å, a N≡N triple bond of 1.103 Å and a ν(NN) stretching frequency red-shifted by −16 cm^{-1} relative to free N_2. Thus, N_2 is not substantially activated in **2V**. It is noteworthy that H_2 is not a better ligand than N_2 for $(\equiv SiO)_2TaH_3$ since the binding energy of H_2 of 1.2 kcal mol^{-1} is also very small (**b** in Scheme 1). Thus, even though **1V** is formally a 10-electron complex, it has little affinity for ligands like N_2 and H_2.

The change in the N_2 coordination from end-on, **2V**, to side-on N_2, **3V** (**c′** in Scheme 1), was calculated to occur via a transition state that is 34.2 kcal mol^{-1} above **2V** ($\Delta G_{298K}^{\ddagger}$ = 31.4 kcal mol^{-1}, $\Delta G_{523K}^{\ddagger}$ = 31.8 kcal mol^{-1}) and is endothermic by 13.4 kcal mol^{-1} (ΔG_{298K} = 15.2 kcal mol^{-1}, ΔG_{523K} = 16.0 kcal mol^{-1}). The change in the coordination of N_2 is concerted with the reductive coupling of the two hydrides to form a dihydrogen ligand. In **3V**, the side-on N_2 ligand has a N−N bond distance of 1.212 Å, significantly longer than in **2V**, and a short average Ta−N bond distance of 2.096 Å (Figure 2). Upon going from the end-on N_2 trihydride, **2V**, to the side-on N_2 dihydrogen monohydride, **3V**, the oxidation state of the metal remains unchanged, and the two electrons originating from the reductive coupling of the two hydrides are used to reduce the dinitrogen ligand to N_2^{2-} as indicated by the significant elongation of the dinitrogen bond distance (from 1.10 to 1.21 Å). A transition state **TS(1V−3V)** for direct side-on coordination to form **3V** from separated **1V** and N_2 was located with an energy of 21.7 kcal mol^{-1} above the separated **1V** and N_2 ($\Delta G_{298K}^{\ddagger}$ = 32.8 kcal mol^{-1}, $\Delta G_{523K}^{\ddagger}$ = 40.5 kcal mol^{-1}; **d** in Scheme 1, Figure 2). Using **1V** as an energy reference, this transition state is lower in energy than **TS(2V−3V)** in which N_2 flips from η^1- to η^2-coordination (**c′** in Scheme 1). At the transition state **TS(1V−3V)**, the two N's are at an equal distance from Ta (2.439(av) Å) with a NN bond distance of 1.141 Å, and the distance between the two hydrogens forming the H_2 ligand is 0.920 Å (Figure 2). This indicates that the side-on coordination of N_2 occurs simultaneously with the formation of a dihydrogen ligand from the reductive coupling of two hydrides, which preserves the d^0 configuration of $Ta^{(V)}$. There are different orientations of the

dx.doi.org/10.1021/ic300498b | Inorg. Chem. 2012, 51, 7237−7249

Scheme 3. Energies and Gibbs Energies at 298 and 523 K (in Parentheses), in kcal mol^{-1}, of Minima and Transition States for the Reactions of 6V and 6′V in the Absence of H_2 (Paths a and a′) and in the Presence of H_2 (Paths b and b′)[a]

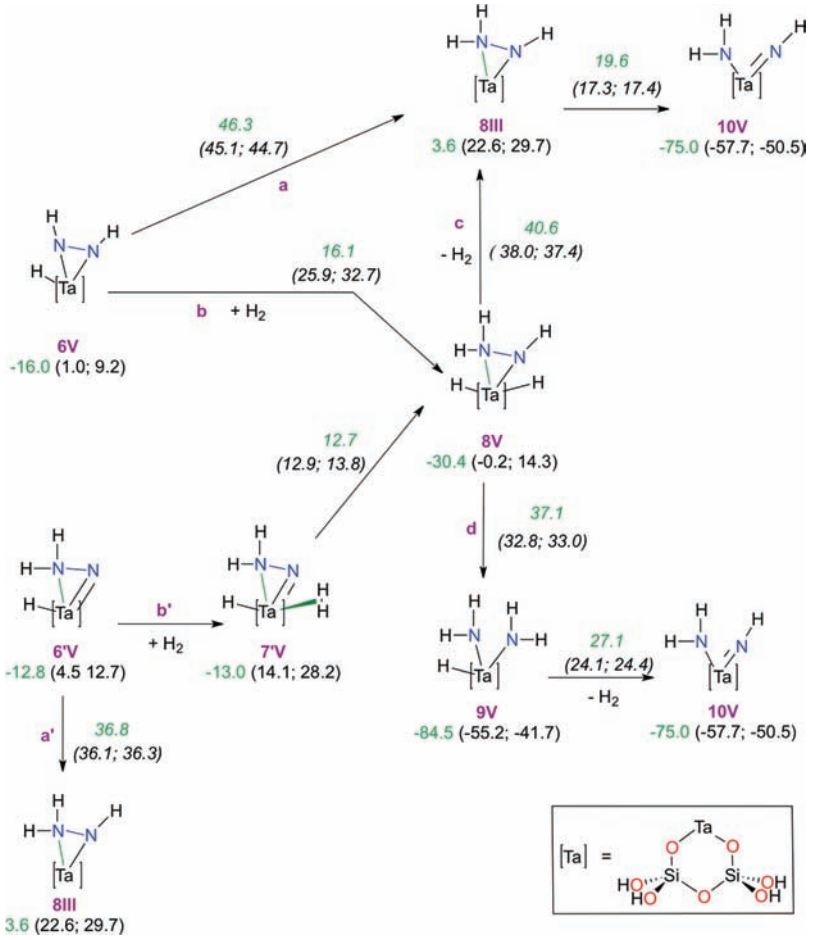

[a]The origin of energies is separated **1V**, H_2 and N_2. A green line between ligand and tantalum represents a ligand-to-metal donor−acceptor bond. The energies and Gibbs energies next to the arrows given in italic are those for the transition state relative the reactant at the start of the arrow. The geometries of all extrema are shown in Figure 4.

N_2 molecule in the transition states of the (**2V** → **3V**) and the (**1V** + N_2 → **3V**) steps. In **TS(2V−3V)**, N_2 is essentially *trans* to a Ta−H bond and almost parallel to the O−Ta−O plane. In **TS(1V−3V)**, N_2 is *trans* to a Ta−O bond and perpendicular to the O−Ta−O plane.

The reaction of N_2 with the monohydride **1III** was also considered (**e** and **f** in Scheme 1). Reaction of **1III** and N_2 led either to the η^1-N_2 complex **2III** or directly to the η^2-N_2 complex **3′V**. The coordination of N_2 is exothermic by −21.8 kcal mol^{-1} (ΔG_{298K} = −9.9 kcal mol^{-1}, ΔG_{523K} = −2.0 kcal mol^{-1}) in the end-on N_2 complex **2III** and by −31.3 kcal mol^{-1} (ΔG_{298K} = −19.7 kcal mol^{-1}, ΔG_{523K} = −11.9 kcal mol^{-1}) in the side-on N_2 complex **3′V**, relative to the separated monohydride complex and N_2, showing a preference for the latter geometry. In **2III**, the Ta−N distance is 2.022 Å, the NN bond distance is 1.141 Å, and the ν(NN) stretching frequency is red-shifted by 405 cm^{-1} relative to free N_2, consistent with a significant back−donation from a formally d^2 $Ta^{(III)}$ center. In **3′V**, the N_2 ligand and the hydride are in the bisector plane of the O−Ta−O angle, and the N−N distance of 1.213 Å together with Ta−N bond lengths of 2.072 and 2.109 Å suggest a $Ta^{(V)}$ metal and a reduced N_2^{2-} ligand (Figure 2). Side-on N_2 coordination to the monohydride complex could be reached either through an experimentally rare η^1- to η^2-coordination flip[44,45] via **TS(2III-3′V)** (**e′** in Scheme 1) or by direct coordination of N_2 to **1III** via **TS(1III-3′V)** (**f** in Scheme 1). The transition states for both steps have similar Gibbs energies relative to the separated **1III** and N_2 ($\Delta G_{298K}^{\ddagger}$ = 12.5 and 12.6 kcal mol^{-1} for **1III** → **3′V** and **2III** → **3′V**, respectively; the correspond-
ing values are 19.1 and 20 kcal mol^{-1} at 523 K). Therefore, calculations suggest that **3′V** could be formed by the addition of N_2 to the monohydride directly, with a rather low energy barrier along step **f** of Scheme 1 or with a higher energy barrier along the steps **e** and **e′** of Scheme 1. Adding H_2 to **3′V** yields **3V**. The transition state for H_2 addition to **3′V** to form **3V** was not searched. The dihydrogen is weakly bonded in **3V** as evidenced by the Ta···H average distance of 2.096 Å, the H−H bond distance of 0.791 Å in **3V**, and the binding energy of 1 kcal mol^{-1}. Therefore, the Gibbs energies of **3V** and **3′V** are determined by the entropic contribution.

In summary, the calculations indicate that dinitrogen can be end-on or side-on bound to the tantalum fragment, which has either one or three atoms of hydrogen. They also indicate that side-on coordinated N_2 can be reached from either the trihydride or the monohydride. Overall, adding nitrogen to the trihydride is slightly endoergic and requires a moderate energy (or Gibbs energy barrier) when passing through **TS(1V−3V)** and a relatively high energy barrier when passing through **TS(2V−3V)**. In contrast, the reaction of dinitrogen with the

dx.doi.org/10.1021/ic300498b | Inorg. Chem. 2012, 51, 7237−7249

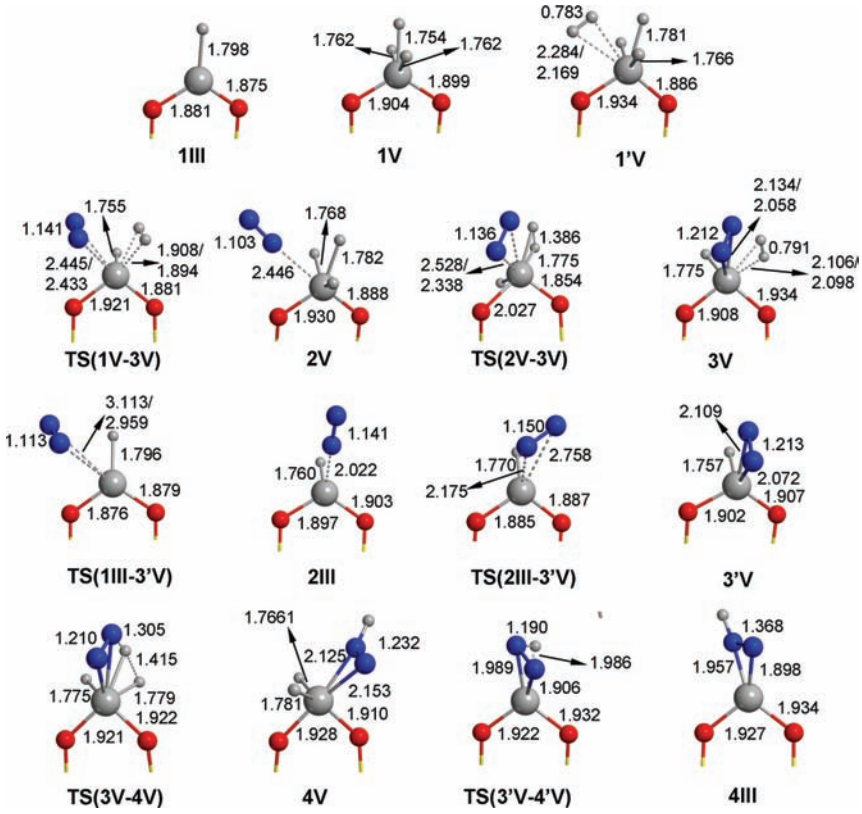

Figure 2. Optimized structures (distances in Å) of extrema associated with the pathways of Scheme 1. The vectors of the imaginary frequencies for the transition states are given in the Supporting Information.

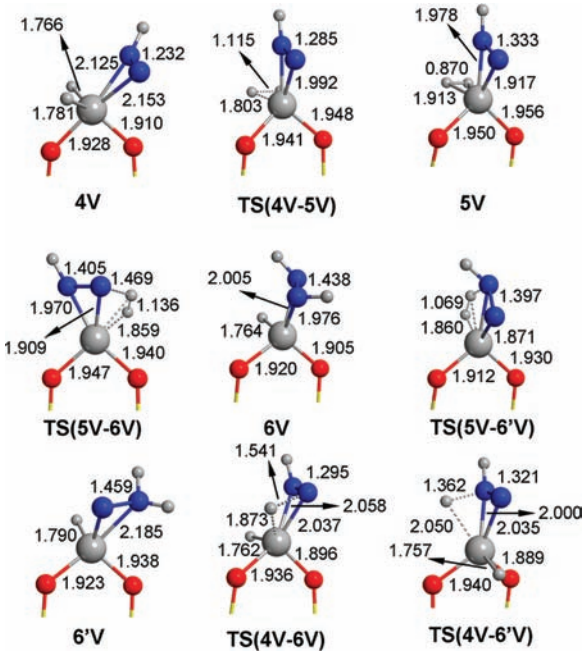

Figure 3. Optimized structures (distances in Å) of extrema associated with the pathways shown in Scheme 2. The vectors of the imaginary frequencies for the transition states are given in the Supporting Information.

monohydride is exoergic (**3'V** relative to **1III** plus N_2) and requires low to modest energy or Gibbs energy barriers (step **f** or **e'** of Scheme 1). The experimental results have shown that N_2 binds to the tantalum center but that there is no insertion of the dinitrogen into a Ta−H bond when a mixture of **1III** and **1V** is exposed to a N_2 atmosphere at room temperature.[24] The only change observed by *in situ* IR spectroscopy upon mixing the tantalum hydride complexes and N_2 at room temperature is attributed to the formation of a weak N_2 complex, as suggested by a ν(NN) stretching frequency of 2280 cm^{-1} (red shift of 51 cm^{-1} relative to free N_2). This result is only compatible with a perturbed but not activated N_2 ligand such as **2V** (calculated red shift of 16 cm^{-1}). In the other N_2 complexes such as **2III**, the calculated ν(NN) stretching frequency is significantly lower (calculated red shift of 405 cm^{-1}), eliminating this species to rationalize the observed IR data. The observed evolution of 0.3 eq/H_2 from the tantalum hydride mixture upon the addition of dinitrogen[24] and the lability of the resulting IR $\nu(N_2)$ band are consistent with the similar energies of **1'V** and **2V** and the low binding energies of the ligands. These results are also consistent with the well-precedented[46] low energy reversible ligand exchange L = H_2 by N_2. The trihydride species appears thus to reversibly coordinate H_2 (**1'V**, **b** in Scheme 1) or N_2 in an atmosphere of H_2 and/or N_2 (**2V**, **c** in Scheme 1), which is in agreement with the similar energies of **1'V** and **2V** relative to **1V** and free H_2 and N_2.

IR monitoring of the reaction of N_2 with the tantalum hydrides does not appear to be the most efficient tool to follow the reaction of the monohydride with N_2 to form **2III** or **3'V** because of the expected low extinction coefficient of side-on dinitrogen adducts[45] and of the existence of stretching $\nu(TaH_x)$ of the starting hydrides and of silica framework deformation bands in the region expected for $\nu(N_2)$ in **2III** and in **3'V** (calculated red shift relative to free N_2 of 405 and 757 cm^{-1}, respectively). However, other data suggest that substantial dinitrogen coordination to tantalum is obtained in the present system. As described in the Experimental Section, the solid resulting from

dx.doi.org/10.1021/ic300498b | *Inorg. Chem.* 2012, 51, 7237−7249

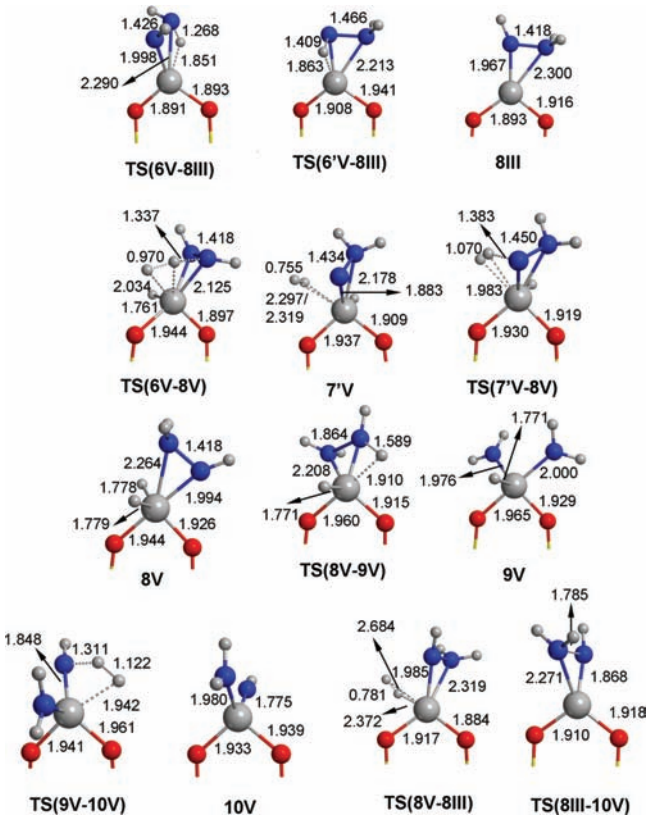

Figure 4. Optimized structures (distances in Å) of extrema associated with the pathways shown in Scheme 3. The vectors of the imaginary frequencies for the transition states are given in the Supporting Information.

exposing a sample of silica-supported tantalum hydrides to a nitrogen atmosphere, enriched in monohydride complexes, has a sizable nitrogen content by combustion analysis (N/Ta ratio = 0.9). This suggests that the N_2 complexes (**2III** and/or **3′V**) are formed from the monohydride, although not observed by IR spectroscopy. These results are in good agreement with the calculations, which indicate that the pathways **1III** → **2III** → **3′V** are energetically accessible.

Formation of $(\equiv SiO)_2TaH_2(N_2H)$. The results are shown in Scheme 1 and Figure 2. Li and Li suggested that complex **3′V** could evolve to $(\equiv SiO)_2Ta(N_2H)$, **4III**, by H transfer to the η^2-coordinated N_2, but this step is endoergic and requires a high activation barrier (>40 kcal mol^{-1}).[28] Experimentally, we have observed that a monohydride $[\equiv SiO)_2TaH]$-enriched sample, when heated at 250 °C under dinitrogen in the absence of H_2, does not give as much intermediate species characterized by $\nu(NH) = 3400$ cm^{-1} as the original mixture of tantalum hydrides under similar conditions. This experimental result (Figure S1) tends to agree with the high energy barrier calculated for the direct N_2 insertion in the Ta−H bond of $(\equiv SiO)_2TaH(\eta^2\text{-}N_2)$. The level of calculations used in this article gives results which are similar to those by Li and Li:[28] The **3′V** → **4III** transformation is endothermic by 17.6 kcal mol^{-1} and the transition state **TS(3′V−4III)** is 41.9 kcal mol^{-1} above **3′V** (**g** in Scheme 1). There are two ways to qualitatively rationalize this high energy barrier: (i) A transfer of a hydride to a highly negatively charged N_2^{2-} ligand is disfavored by the high energy of the empty ligand orbitals (more later in the discussion) and also because of unfavorable electrostatic interactions. (ii) The transfer can be viewed as a reductive H transfer in which a proton is added to N_2^{2-}, and thus, the metal is reduced from $Ta^{(V)}$ to $Ta^{(III)}$, a relatively unfavorable oxidation state for the metal. Therefore, although the reaction takes place at 250 °C and is compatible with high-energy barrier elementary steps, we have searched for alternative energetically more accessible pathways.

In **3V**, there are two different types of hydrogen. While the hydrogen directly bonded to Ta is a hydride, the dihydrogen ligand coordinated to a metal has acidic character.[30] Therefore, considering that N_2 is negatively charged in **3V**, it is more likely to react with the electron-poor hydrogen of coordinated H_2. The transition state for the heterolytic cleavage of H_2 with the proton being transferred to the coordinated dinitrogen is shown in Figure 2. The **TS(3V−4V)** transition state is calculated to be 15.3 kcal mol^{-1} above **3V** ($\Delta G_{298K}^{\ddagger}$ = 13.9 kcal mol^{-1}, $\Delta G_{523K}^{\ddagger}$ = 14.2 kcal mol^{-1}), and it yields **4V**, which is essentially isoergic with **3V** (**h** in Scheme 1). At the transition state **TS(3V−4V)**, the N···H···H angle is 150°, and the tantalum center, the two nitrogen, and the two hydrogen atoms are coplanar. This geometry is characteristic of a proton transfer from the acidic dihydrogen ligand to one of the N lone pairs of the N_2^{2-} ligand. The product, **4V**, has the two hydrides separated by a distance of more than 3 Å and an η^2-N_2H ligand. This ligand has a N−N−H angle of 120.3° and a N−N bond distance of 1.232 Å; it is thus well described as a $[N{=}NH]^-$ ligand. In the **3V** → **4V** transformation, the oxidation state of tantalum does not change, and the dinitrogen ligand goes from N_2^{2-} to N_2H^- upon the transfer of the proton.

Formation of $(\equiv SiO)_2TaH(N_2H_2)$. The results are shown in Scheme 2 and Figure 3. After the formation of **4V**, a second H transfer to the N_2H ligand is necessary. The energetics of all possible H transfers to **4V** are shown in Scheme 2. Since the N_2H ligand formally carries a single negative charge, it could still prefer to react with a positively charged species. However, a reaction with a negatively charged hydride should not be as unfavorable as for the **3′V** → **4III** transformation (**g** in Scheme 1). We have explored all possibilities (paths **b** + **c** or **b** + **c′** and paths **d** or **d′** in Scheme 2). To induce the first path, which involves a proton transfer, there is a need for a dihydrogen in the coordination sphere. Since **4V** is hexacoordinated, the addition of H_2 is not possible; the formation of the dihydrogen complex **5V** can occur by reductive coupling of the hydrides present in **4V**. The dihydrogen adduct **5V** is 8.2 kcal mol^{-1} above **4V** and is reached with an energy barrier of 9.3 kcal mol^{-1} (ΔG_{523K} = 8.1 kcal mol^{-1}, $\Delta G_{523K}^{\ddagger}$ = 9.0 kcal mol^{-1}; **b** in Scheme 2). From **4V** to **TS(4V−5V)** to **5V**, the N−N bond distance in the N_2H ligand lengthens from 1.232 to 1.285 and to 1.335 Å, and the H···H distance shortens from 3.039 Å to 1.115 and to 0.870 Å (Figure 3). The long NN bond distance in **5V** is thus intermediate between that of a single and that of a double NN bond, which is indicative of either a significant back-donation from a $Ta^{(III)}$ to $[N_2H]^-$ ligand or a significant donation of electron density from a fully reduced $[N_2H]^{3-}$ ligand to a $Ta^{(V)}$ center.[47] In parallel, some additional electron density is also present on the coordinated H_2 ligand of **5V**, as indicated by the H−H bond distance of 0.870 Å. The two ways to consider the electronic structure of **5V** indicate that the reductive coupling of the two hydrides has accumulated considerable density on the HN−N ligand, while some still remains in the coordinated H_2.

From **5V**, the heterolytic cleavage of H_2 can occur across one of the two Ta−N bonds of the N_2H ligand (**c** and **c′** in Scheme 2). The two steps have similar and relatively low energy barriers ($\Delta E^{\ddagger}$ = 8.2 and 9.8 kcal mol^{-1} for **c** and **c′**, respectively), and they are both highly exothermic (ΔE around −30 kcal mol^{-1}).

dx.doi.org/10.1021/ic300498b | Inorg. Chem. 2012, 51, 7237−7249

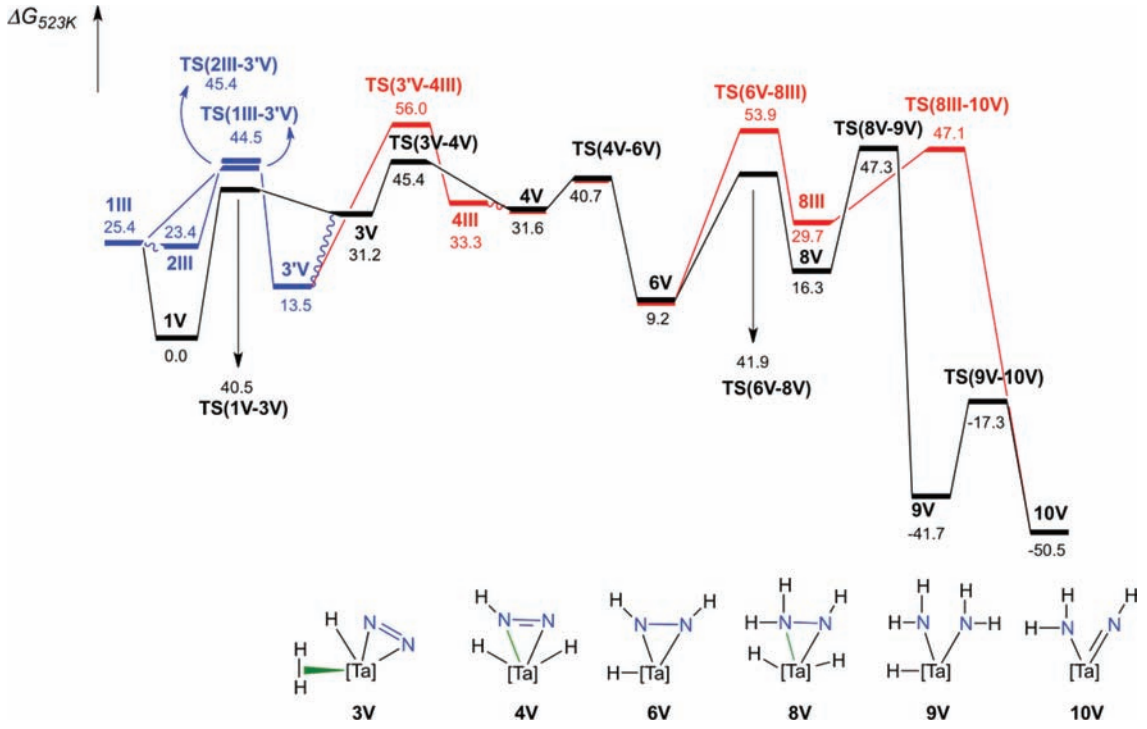

Figure 5. Gibbs energy profiles (in kcal mol^{-1}) at 523 K for the reaction of N_2 and H_2 in the presence of silica supported tantalum hydrides ($\equiv SiO)_2TaH_x$ (x = 1, **1III** and x = 3, **1V**) to form the amido imido Ta(V) ($\equiv SiO)_2Ta(NH)(NH_2)$ complex **10V**. The pathways implying isomer **6′V** are not reported for clarity (the overall energy is similar to the route implying **6V**). Likewise, the alternative **4V** → **6V** step going through **5V** is not reported. See Schemes 1−3 for details on each step and label assignments, and see Figures 2−4 for geometries of all extrema. A green line between ligand and tantalum represents a ligand-to-metal donor−acceptor bond. [Ta] represents the silica supported tantalum species.

The transition states for **5V** to **6V** and **5V** to **6′V** have distances between the two hydrogens slightly longer than 1 Å and H···H···N angles of 130° and 151°, respectively, compatible with a proton transfer between ligands with geometrical constraints in their bonds to tantalum. In **6V** and **6′V**, the N−N bond distances are similar and longer than 1.43 Å, indicative of a N−N single bond. As a consequence, in both **6V** and **6′V**, the nitrogen-based ligand is best described as $[N_2H_2]^{2-}$, stabilized by a $Ta^{(V)}$ center.

The alternative pathways to form **6V** and **6′V** from **4V** are by the direct hydride transfer to the $[HN{=}N]^-$ (**d** and **d′** in Scheme 2). In contrast with what was obtained for the H_2 heterolytic cleavage routes, **5V** → **6V** (**b** + **c** in Scheme 2) and **5V** → **6′V** (**b** + **c′** in Scheme 2), for which protonation of the two ends of the N_2H ligand have similar energy barriers, the hydride transfers in **4V** to form **6V** and **6′V** (**d** and **d′** in Scheme 2) have different energy barriers. The hydride transfer to form the symmetrical HNNH ligand has an energy barrier of 8.6 kcal mol^{-1} above **4V**, while the corresponding value to form **6′V** is 33.4 kcal mol^{-1} ($\Delta G_{523K}^{\ddagger}$ = 9.1 and 34.2 kcal mol^{-1}, respectively). This difference in the energy barriers between these two paths is not easy to understand, but similar results were reported by Li and Li.[28]

Overall, the formation of **6V** could be obtained either via direct hydride transfer (**d** in Scheme 2) or by proton transfer after intramolecular formation of a dihydrogen complex (**b** + **c** in Scheme 2). Unlike the **3′V** → **4III** step described in the previous section, the direct hydride transfer to the $[N_2H]^-$ ligand to form $[N_2H_2]^{2-}$ (**4V** → **6V**) does not have a high-energy barrier. In **TS(4V−6V)**, the hydride adds to the π system of coordinated N_2H that is perpendicular to the Ta−N−N plane (N−N distance = 1.295 Å, N···hydride distance = 1.541 Å, H−N−N···hydride dihedral angle = 100°; Figure 3). The π^* orbital of the HN═N ligand is well suited for interacting with a hydride, and the formally single negatively charged $[HN{=}N]^-$ ligand is more electrophilic than the doubly negatively charged N_2^{2-} in **3′V**.

The pathways **4V** → **6V** or **6′V** via initial dihydrogen formation (**5V**) followed by proton transfer to the N_2H ligand of **5V** (**b** + **c** or **b** + **c′** in Scheme 2) are energetically equivalent to the direct hydride transfer, **4V** to **6V**. Thus, one could expect that **6V** is formed via either hydride transfer or by dihydrogen formation followed by proton transfers (**d** or **b** + **c** in Scheme 2, respectively) but that **6′V** is formed via dihydrogen formation followed by proton transfer (**b** + **c′** in Scheme 2).

Reaction of ($\equiv$SiO)$_2$TaH(N$_2$H$_2$) in the Absence and in the Presence of Additional H$_2$. The results are given in Scheme 3 and Figure 4. The transfer of the hydride to the $[N_2H_2]^{2-}$ ligand in **6V** or to the $[NNH_2]^{2-}$ ligand in **6′V** could lead to the final amido imido $Ta^{(V)}$ complex if the hydride transfer were concerted with N−N bond cleavage. Neither Li and Li[28] nor have we observed such a direct mechanism. Li and Li have suggested that the transformation of **6V** or **6′V** to the final amido−imido $Ta^{(V)}$ complex, **10V**, occurs by hydride transfer followed by the cleavage of the remaining bond between the two nitrogen atoms, in two sequential steps. The hydride transfer step has an especially high energy barrier and is endoergic.[28] We have obtained essentially the same results (**a** and **a′** in Scheme 3). The **6V** → **8III** and **6′V** → **8III** transformation are endothermic by 19.6 and 16.4 kcal mol^{-1}, respectively, and the associated energy barriers are 46.3 kcal mol^{-1} ($\Delta G_{523K}^{\ddagger}$ = 44.7 kcal mol^{-1}) from **6V** and 36.8 kcal mol^{-1} ($\Delta G_{523K}^{\ddagger}$ = 36.3 kcal mol^{-1}) from **6′V**.

Since the hydride transfer to go from **6V** to **8III** has a high-energy barrier, we have explored alternative pathways, which could involve a proton transfer. This requires the participation of

dx.doi.org/10.1021/ic300498b | Inorg. Chem. 2012, 51, 7237−7249

an additional molecule of H_2. This dihydrogen adds across the Ta−N bond of **6V** to form $(\equiv SiO)_2TaH_2(N_2H_3)$, **8V**, with an energy barrier of 16.1 kcal mol^{-1} (**b** in Scheme 3). This heterolytic addition of H_2, which takes place without prior coordination of dihydrogen to the metal, is exothermic by $\Delta E = -14.4$ kcal mol^{-1} relative to **6V**. In the reaction of H_2 with **6′V** (**b′** in Scheme 3), a H_2 adduct, **7′V**, was located prior to the addition across the un-hydrogenated Ta═N bond. The transition states for **7′V** + H_2 → **8V** and for **6V** + H_2 → **8V** have similar energies and Gibbs energies. These transition states have a structure that indicates that a proton is transferred to the nitrogen atom (in **TS(6V−8V)**, the N···H and H···H distances are 1.337 and 0.970 Å, respectively) while a Ta−H bond is formed (Ta···H distance of 2.034 Å; Figure 4). They resemble the transition state for the **3V** → **4V** transformation, which is shown in Figure 2. In **8V**, the two hydrides are far from each other (3.170 Å), and the NN bond distance in the $NHNH_2^-$ ligand is 1.418 Å. The addition of a proton to the $[N_2H_2]^{2-}$ ligand in **6V** or **6′V** is thus energetically easier than the intramolecular hydride transfer, but it requires the participation of an additional dihydrogen molecule. These results suggest that the reaction should stop at the formation of **6V** and **6′V** in the absence of available H_2. This result rationalizes an important experimental observation. IR spectroscopy monitoring after heating a sample of the $(\equiv SiO)_2TaH_x$ mixture exposed only to N_2 shows a substantial decrease of the $\nu(Ta-H_x)$ stretching bands, suggesting that a reaction has occurred between N_2 and the silica supported tantalum hydride complexes, but very little final product is observed.[24] Nevertheless, significant amounts of the final product are observed when H_2 is added to the reactive media and the system is heated.[24]

Formation of $(\equiv SiO)_2Ta(NH)(NH_2)$. The results are shown in Scheme 3 and Figure 4. Reductive elimination of H_2 from **8V** yields the $Ta^{(III)}$ complex **8III** (**c** in Scheme 3). This transformation, which is strongly endoergic and requires a high-energy barrier, is unlikely to occur. The hydride transfer to the NH_2NH^- ligand transforms **8V** into a bisamido $Ta^{(V)}$ complex **9V** when H is added to the NH end (**d** in Scheme 3), and it leads to an ammonia imido $Ta^{(V)}$ complex **9′V** (not shown in Scheme 3 and Figure 4) if the hydride adds to the NH_2 end. Nevertheless, attempts to locate the transition state for the latter case were not successful. Note that **9′V** is 5.3 kcal mol^{-1} higher in energy than **9 V**.[34] The **TS(8V−9V)** transition state is 37.1 kcal mol^{-1} above **8V** ($\Delta G_{523K}^{\ddagger}$ = 33.0 kcal mol^{-1}), but the reaction is strongly exothermic since **9V** is 54.1 kcal mol^{-1} below **8V** ($\Delta G_{523K} = -56.0$ kcal mol^{-1}). The energy barrier for the **8V** → **9V** step is slightly lower than that for **8V** → **8III**. The two transition states have similar energies, but there is a large thermodynamic preference for cleaving the NN bond via hydride addition to the ligand over eliminating H_2 without cleaving the NN bond. At the transition state **TS(8V−9V)**, the hydrogen is 1.589 Å from the NH nitrogen; the N−N···H angle is 139°; and the two nitrogen, the tantalum, and the hydrogen atoms are coplanar (Figure 4). The NN bond distance is 1.864 Å, which is thus significantly longer than in **8V** (1.418 Å). These geometrical features show that the hydrogen is interacting with the empty σ^*_{NN} orbital. Therefore, the reaction is best viewed as a hydride addition to the NH end of the NH_2NH^- ligand. The bisamido hydride $Ta^{(V)}$ complex **9V** has been previously described.[34] It is noteworthy that this is the first species among all minima located for N_2 hydrogenation that has a Gibbs energy at 523.15 K lower than that of the reactants because the loss of the strong NN bond is compensated by the formation of two strong Ta−amido bonds.

The **9V** intermediate can evolve to the final product **10V** through a heterolytic loss of H_2. This elementary step has been found to be part of the pathway for the experimentally observed H exchange in the reaction of **10V** with H_2.[33] This transformation is the reverse reaction of the heterolytic addition of H_2 to the Ta−N bond described in the **6V** → **8V** transformation. Therefore, the final product **10V** is formed after elimination of a H_2 molecule, while H_2 had been added to **6V** two elementary steps earlier to favor the hydrogenation of $HNNH^{2-}$ or NH_2N^-. The heterolytic elimination is slightly endothermic by 9.5 kcal mol^{-1}, and involves an energy barrier of 27.1 kcal mol^{-1}. However, the loss of H_2 is entropically favorable, and this leads to **10V** and free H_2 having a lower Gibbs energy than **9V**, both at room temperature and at 250 °C by 2.6 and 8.8 kcal mol^{-1}, respectively.

DISCUSSION

Figure 5 shows the complete Gibbs energy profile at 523 K associated with the sequence of elementary steps that yield the formation of the amido−imido $Ta^{(V)}$ complex from the initial silica-grafted tantalum trihydride mixture, N_2 and H_2. The corresponding potential energy profile using E is shown in the Supporting Information (Figure S3). The overall shapes are similar, but the lack of the entropic contribution in the latter prevents proper representation of the association and dissociation processes. Even though the calculations of the entropy contributions are not accurate with the method used (see Computational Details), it is preferable to consider the Gibbs energy profile to have a qualitative description of the global process.

Li and Li have calculated a full mechanism with the B3LYP[36,48] functional.[28] The extrema found by them have been also calculated with our method of calculation (B3PW91), and they are shown in the red curve in Figure 5. Since the two methodologies give essentially the same results, we can compare the pathway proposed by Li and Li (red curve) using our energy values to the alternative pathway (black curve).

The preferred pathway that emerges from our calculations is described as follows. The tantalum trihydride (**1V**) and the separated monohydride (**1III**) can bind N_2. The end-on coordination is kinetically easy but leads to an unactivated dinitrogen ligand. For the monohydride, the side-on coordination has a lower energy barrier but leads to the $(\equiv SiO)_2TaH(\eta^2\text{-}N_2)$ complex, **3′V**, inert toward N_2 insertion in the Ta−H bond. Its further reactivity is possible by the addition of H_2 to give $TaH(N_2)(H_2)$, **3V**, an intermediate of the trihydride N_2 reduction route (*vide infra*). The trihydride reduction route becomes thus the most relevant. The preferred pathway to reach a side-on η^2-N_2 coordination directly from the trihydride is to associate the addition of N_2 with the reductive coupling of two hydrides, **TS(1V−3V)**, in a concerted manner. This yields the monohydride dihydrogen dinitrogen $Ta^{(V)}$ complex mentioned above (**3V**) in which the N_2 has been strongly activated by becoming N_2^{2-}. In this way, one of the two π-bonds of N_2 is broken. The next step is a proton transfer from the coordinated H_2 to the activated nucleophilic N_2^{2-} ligand via **TS(3V−4V)**, which is followed by a hydride transfer via **TS(4V−6V)** to the other nitrogen. The hydride transfer cleaves the second π-bond and forms $[HNNH]^{2-}$ (the formation of $[NNH_2]^{2-}$ is also possible and represents an alternative pathway). Once $[HNNH]^{2-}$ is formed, there is only one hydride left on the tantalum complex. The addition of this remaining hydride to the σ^*_{NN} orbital of $[HNNH]^{2-}$ via **TS(6V−8III)** requires a high-energy barrier.

dx.doi.org/10.1021/ic300498b | Inorg. Chem. 2012, 51, 7237−7249

An alternative path with a significantly lower activation barrier exists: it entails the heterolytic addition of molecular dihydrogen across the Ta−N bond via **TS(6V−8V)**. This protonation is followed by a hydride transfer that cleaves the σ N−N bond of $[H_2NNH]^-$ via **TS(8V−9V)**. The final step proceeds via **TS(9V−10V)** and consists of the heterolytic elimination of dihydrogen that forms the final amido−imido $Ta^{(V)}$ complex. These elementary steps show that the transformation from the $[HNNH]^{2-}$ complex to the final product is assisted by H_2, which is fully recovered at the end of this transformation, and that the cleavage of the σ bond of the $[HNNH]^{2-}$ ligand by way of hydride transfer is significantly more difficult.

The transition states of the pathway proposed in this study (black curve, Figure 5) are lower in Gibbs energy than those proposed by Li and Li (red curve). The difference in Gibbs energy between the two highest transition structures is around 9 kcal mol^{-1}. Even though the temperature used in the experiment is high (250 °C), this difference in energy between the two highest transition states is significant. The two pathways differ in that the one presented in this work avoids the hydride transfer to a formally doubly charged ligand. Even if counting the number of electrons assigned to ligands is somewhat arbitrary and only done here in a qualitative manner, it is well supported by the structural features and in particular by the NN bond distance which parallels the number of NN π bonds.[47] A hydride transfer to a strongly negatively charged ligand is made unfavorable by the electrostatic repulsion between the two groups and by the high-energy level of its empty orbitals. A way to circumvent the difficulty is to react the ligand with a proton. This reduces the formal charge by one and lowers the energy of the empty orbitals of the ligand, which makes the later addition of a hydride more probable. This process is somewhat related to the proton induced electron transfer with the difference that the electrons are associated with the hydrogen nucleus.[49] This succession of proton and hydride transfers occurs twice in the whole reaction. In the two occurrences, the proton originates from H_2, either coordinated on the metal center, which renders the H_2 ligand acidic, or by the heterolytic addition of H_2 to a polar Ta−N bond. The protonation of the metal-coordinated N_2 moiety by a similarly metal-coordinated dihydrogen has several precedents implying bimetallic systems.[10,20] In the system studied here, the proton transfer occurs on a single metal atom. In the second case, H_2 is heterolytically added before being eliminated also in a heterolytic manner. By leading to lower energy barriers and by being fully recovered, H_2 appears as assisting the final steps of the reaction. Therefore, molecular hydrogen has been used as the source of protons and electrons due to the ability of the metal and ligands in this system to promote its heterolytic cleavage provided that an empty coordination site at the metal is available to host the hydride. It is probably this low coordinated state of the tantalum on the silica surface which makes all these steps possible.

Experimental work shows that exposing the tantalum sites to a hydrogen-free N_2 atmosphere at room temperature leads some of the tantalum sites to coordinate dinitrogen reversibly with concomitant dihydrogen elimination. A measured $\nu(N_2)$ stretching band of 2280 cm^{-1} in the IR spectrum at room temperature is suggestive of a dinitrogen weakly influenced by coordination (red shift of 51 cm^{-1} from free N_2).[7,50] Calculations show that coordination to the trihydride leads to a red shift of 16 cm^{-1}. The calculations show that end-on coordination of N_2 to the monohydride species gives a red shift of 405 cm^{-1}, which excludes this species as being the one observed. All side-on N_2 coordination gives much larger red shifts ($\Delta\nu < -750$ cm^{-1}) and should in principle be silent to IR spectroscopy. Thus, all of these data suggest that the trihydride can weakly coordinate N_2 even if it is unclear how the weak binding energy can overcome the entropy cost of the coordination.

Heating the mixture at 250 °C leads to the disappearance of the Ta−H stretching frequencies and the appearance of stretching frequencies in the N−H region but not to the full conversion to the final product. Calculations suggest that the experimentally observed intermediates could be **6V** or **6′V**, which contain $[HNNH]^{2-}$ and $[NNH_2]^{2-}$ ligands, respectively. The calculated unscaled ν(NH) frequencies in **6V** and **6′V** are between 3566 and 3468 cm^{-1}, which are reasonably close to the band observed around 3400 cm^{-1}. It is noteworthy that, while the Gibbs energies of **6V** and **6′V** are higher than that of the starting reactants at 250 °C, they become isoergic at room temperature, giving a potential explanation on why they are observed. All other intermediates still having some NN bond are predicted to be significantly higher in Gibbs energy at room temperature. Moreover, the experimental data suggest that these observed intermediates cannot evolve to products in the absence of additional H_2. This is rationalized by the calculations which show that the preferred path is via **TS(6V−8V)** rather than via **TS(6V−8III)**.

The strong preference of tantalum for a high oxidation state tends to localize the electron density on the ligands if they have available empty orbitals. In the pathway that is proposed in this paper, the tantalum remains in its preferred $Ta^{(V)}$ high oxidation state. Additional electron density is provided by using the hydrides when needed. For instance, reductive coupling of the hydrides does not reduce the metal but the dinitrogen ligand. This ligand-to-ligand electron transfer is only possible with a very electropositive metal that strongly favors a high oxidation state. Another requirement for the reaction to proceed is the presence of more than one empty coordination site to allow the coordination of N_2 and H_2. In the present case, the tantalum center, immobilized on the surface and coordinated to poor electron donor ligands like the siloxy groups is able to fulfill the required specification, but this does not seem to be specific to Ta. Thus, other early 4d and 5d metals with the appropriate ligands may be able to achieve related transformations. We are exploring these possibilities further.

CONCLUSIONS

A reaction pathway for the reaction of N_2 and H_2 with silica-supported tantalum hydrides complexes to form an amido−imido tantalum complex has been proposed. By invoking the possibility of transfer of protons from dihydrogen to the various nitrogen-based ligands formed during the reaction to increase their electrophilicity, it is shown that N_2 can be reduced by hydride transfers or two-electron reduction all the way to the amido−imido ligands. The dihydrogen is thus the source of protons and electrons, possibly, by way of hydride transfers. This behavior of dihydrogen is made possible by the electropositive tantalum, which makes a coordinated H_2 molecule a reasonable proton donor and the presence of strongly polar Ta−N bonds that favor the heterolytic cleavage of H_2. In this reaction, the tantalum remains in its preferred high oxidation state and avoids redox-type reactions, which could be energetically demanding. An important requirement for the reaction to proceed is that the metal is unsaturated to allow the coordination of N_2 and H_2. This is the case in this study where the tantalum center is immobilized on a surface and coordinated to poor electron donor ligands like the siloxy groups.

dx.doi.org/10.1021/ic300498b | Inorg. Chem. 2012, 51, 7237−7249

■ ASSOCIATED CONTENT

Supporting Information

Infrared spectra of N_2 addition and heating to tantalum hydrides. Graphical representation of the vectors associated with the imaginary frequencies for all transition states. Potential energy profile of the proposed mechanism with B3PW91 functional. Energies and Gibbs energies at 298 K of minima and transition states computed with the M06 functional. List of coordinates of all calculated extrema, with their absolute Energies E and Gibbs energies with B3PW91 (298 and 523 K) and M06 (298 K) functionals. The material is available free of charge via the Internet at http://pubs.acs.org.

■ AUTHOR INFORMATION

Corresponding Author

*E-mail: xavi@klingon.uab.es, jeanmarie.basset@kaust.edu.sa, quadrelli@cpe.fr, Odile.eisenstein@univ-montp2.fr.

Present Addresses

[‖]Department of Chemistry, Chemistry Department, University of British Columbia, 2036 Main Mall, Vancouver, Canada V6T 1Z1

[⊥]Leiden Institute of Chemistry, Universiteit Leiden, P.O. Box 9502, 2300 RA Leiden, The Netherlands

[#]Kaust Catalysis Center, King Abdullah University of Science and Technology, Thuwal 23955-6900, Saudi-Arabia

Notes

The authors declare no competing financial interest.

■ ACKNOWLEDGMENTS

E.A.Q. thanks the French national research agency for a research grant (ANR JC08_326469). X.S.-M. thanks the support of the Generalitat de Catalunya (Project SGR2009-638) and the MEC/MICINN of Spain (CTQ2011-24847/BQU) as well as the Ramón y Cajal fellowship at the end of the project. O.E. thanks the Ministère de l'Enseignement Supérieur et de la Recherche and the CNRS for funding. X.S.-M. thanks Dr. G. Ujaque (UAB) for fruitful discussions.

■ REFERENCES

(1) Crookes, W. *Report of the 68th meeting of the British Association for the Advancement of Science Bristol 1898*; John Murray: London, 1898; p 3.

(2) (a) Ertl, G. *Catalytic Ammonia Synthesis*; Jennings, J. R., Ed.; Plenum Press: New York, 1991. (b) Appl, M. *Ammonia: Principles and Industrial Practice*; Wiley-VCH: Weinheim, Germany, 1999. (c) Postgate, J. *Nitrogen Fixation*, 3rd ed.; Cambridge University Press: Cambridge, U. K., 1998.

(3) (a) Howard, J. B.; Rees, D. C. *Chem. Rev.* **1996**, *96*, 2965−2982. (b) Burgess, B. K.; Lowe, D. J. *Chem. Rev.* **1996**, *96*, 2983−3011. (c) Smith, B. E. *Adv. Inorg. Chem.* **1999**, *47*, 159−218. (d) Rees, D. C.; Howard, J. B. *Curr. Opin. Chem. Biol.* **2000**, *4*, 559−566. (e) Barney, B. M.; Lee, H. I.; Dos Santos, P. C.; Hoffman, B. M.; Dean, D. R.; Seefeldt, L. C. *Dalton Trans.* **2006**, 2277−2284. (f) Howard, J. B.; Rees, D. C. *Proc. Natl. Acad. Sci. U. S. A.* **2006**, *103*, 17088−17093. (g) Barrière, F. *Coord. Chem. Rev.* **2003**, *236*, 71−89. (h) Dance, I. *Dalton Trans.* **2010**, *39*, 2972−2983. (i) Hinnemann, B.; Nørskov, J. K. *J. Am. Chem. Soc.* **2004**, *126*, 3920−3927.

(4) (a) Schlögl, R. *Angew. Chem., Int. Ed.* **2003**, *42*, 2004−2008. (b) Schlögl, R. *Handbook of Heterogeneous Catalysis*; Ertl, G., Knözinger, H., Schüth, F., Weitkamp, J., Eds.; Wiley VCH Verlag: Weinheim, Germany, 2008; Vol. 5, pp 2501−2575. (c) Forni, L. *Chem. Ind.* **2009**, *91*, 108−112.

(5) (a) Ertl, G. *Angew. Chem., Int. Ed.* **2008**, *47*, 3524−3535. (b) Shetty, S.; Jansen, A. P. J.; van Santen, R. A. *J. Phys. Chem. C* **2008**, *112*, 17768−17771.

(6) Hellman, A.; Baerends, E. J.; Biczysko, M.; Bligaard, T.; Christensen, C. H.; Clary, D. C.; Dahl, S.; van Harrevelt, R.; Honkala, K.; Jonsson, H.; Kroes, G. J.; Luppi, M.; Manthe, U.; Nørskov, J. K.; Olsen, R. A.; Rossmeisl, J.; Skúlason, E.; Tautermann, C. S.; Varandas, A. J. C.; Vincent, J. K. *J. Phys. Chem. B* **2006**, *110*, 17719−17735.

(7) For selective reviews, see for instance: (a) MacKay, B. A.; Fryzuk, M. D. *Chem. Rev.* **2004**, *104*, 385−401. (b) Gambarotta, S.; Scott, J. *Angew. Chem., Int. Ed.* **2004**, *43*, 5298−5308. (c) Schrock, R. R. *Proc. Natl. Acad. Sci. U. S. A.* **2006**, *103*, 17087−17087. (d) Hazari, N. *Chem. Soc. Rev.* **2010**, *39*, 4044−4056.

(8) Allen, A. D.; Senoff, C. V. *Chem. Commun.* **1965**, 621−622.

(9) Chatt, J.; Leigh, G. J. *Chem. Soc. Rev.* **1972**, *1*, 121−144.

(10) Nishibayashi, Y.; Iwai, S.; Hidai, M. *Science* **1998**, *279*, 540−542.

(11) (a) Nishibayashi, Y.; Takemoto, S.; Iwai, S.; Hidai, M. *Inorg. Chem.* **2000**, *39*, 5946−5957. (b) Hidai, M.; Mizobe, Y. *Chem. Rev.* **1995**, *95*, 1115−1133.

(12) (a) Shilov, A. E. *Russ. Chem. Bull.* **2003**, *52*, 2555−2562. (b) Bazhenova, T. A.; Shilov, A. E. *Coord. Chem. Rev.* **1995**, *144*, 69−145.

(13) (a) Yandulov, D. V.; Schrock, R. R. *Science* **2003**, *301*, 76−78. (b) Ritleng, V.; Yandulov, D. V.; Weare, W. W.; Schrock, R. R.; Hock, A. S.; Davis, W. M. *J. Am. Chem. Soc.* **2004**, *126*, 6150−6163. (c) Yandulov, D. V.; Schrock, R. R. *Inorg. Chem.* **2005**, *44*, 5542−5542. (d) Schrock, R. R. *Acc. Chem. Res.* **2005**, *38*, 955−962. (e) Weare, W. W.; Dai, X. L.; Byrnes, M. J.; Chin, J. M.; Schrock, R. R.; Müller, P. *Proc. Natl. Acad. Sci. U. S. A.* **2006**, *103*, 17099−17106.

(14) Arashiba, K.; Miyake, Y.; Nishibayashi, Y. *Nature Chem.* **2011**, *3*, 120−125.

(15) (a) Pickett, C. J.; Talarmin, J. *Nature* **1985**, *317*, 652−653. (b) Murakami, T.; Nishikiori, T.; Nohira, T.; Ito, Y. *J. Am. Chem. Soc.* **2003**, *125*, 334−335. (c) Marnellos, G.; Stoukides, M. *Science* **1998**, *282*, 98−100. (d) Pospíšil, L.; Buličková, J.; Hromadová, M.; Gál, M.; Civiš, S.; Cihelka, J.; Tarábek, J. *Chem. Commun.* **2007**, 2270−2272. (e) Skúlason, E.; Bligaard, T.; Gudmundsdottir, S.; Studt, F.; Rossmeisl, J.; Abild-Pedersen, F.; Vegge, T.; Jonsson, H.; Norskøv, J. K. *Phys. Chem. Chem. Phys.* **2012**, *14*, 1235−1245.

(16) Rao, N. N.; Dube, S.; Manjubala; Natarajan, P. *Appl. Catal., B* **1994**, *5*, 33−42.

(17) Rodriguez, M. M.; Bill, E.; Brennessel, W. W.; Holland, P. L. *Science* **2011**, *334*, 780−783.

(18) (a) Himmel, H. J.; Hübner, O.; Klopper, W.; Manceron, L. *Angew. Chem., Int. Ed.* **2006**, *45*, 2799−2802. (b) Himmel, H. J.; Reiher, M. *Angew. Chem., Int. Ed.* **2006**, *45*, 6264−6288. (c) Lu, Z. H.; Jiang, L.; Xu, Q. *J. Phys. Chem. A* **2010**, *114*, 6837−6842.

(19) (a) Solari, E.; Da Silva, C.; Iacono, B.; Hesschenbrouck, J.; Rizzoli, C.; Scopelliti, R.; Floriani, C. *Angew. Chem., Int. Ed.* **2001**, *40*, 3907−3909. (b) Clentsmith, G. K. B.; Bates, V. M. E.; Hitchcock, P. B.; Cloke, F. G. N. *J. Am. Chem. Soc.* **1999**, *121*, 10444−10445. (c) Korobkov, I.; Gambarotta, S.; Yap, G. P. A. *Angew. Chem., Int. Ed.* **2002**, *41*, 3433−3436. (d) Korobkov, I.; Gambarotta, S.; Yap, G. P. A. *Angew. Chem., Int. Ed.* **2003**, *42*, 4958−4961. (e) Nikiforov, G. B.; Vidyaratne, I.; Gambarotta, S.; Korobkov, I. *Angew. Chem., Int. Ed.* **2009**, *48*, 7415−7419. (f) Vidyaratne, I.; Crewdson, P.; Lefebvre, E.; Gambarotta, S. *Inorg. Chem.* **2007**, *46*, 8836−8842. (g) Vidyaratne, I.; Scott, J.; Gambarotta, S.; Budzelaar, P. H. M. *Inorg. Chem.* **2007**, *46*, 7040−7049. (h) Laplaza, C. E.; Cummins, C. C. *Science* **1995**, *268*, 861−863. (i) Laplaza, C. E.; Johnson, M. J. A.; Peters, J. C.; Odom, A. L.; Kim, E.; Cummins, C. C.; George, G. N.; Pickering, I. J. *J. Am. Chem. Soc.* **1996**, *118*, 8623−8638. (j) Fryzuk, M. D.; Kozak, C. M.; Bowdridge, M. R.; Patrick, B. O.; Rettig, S. J. *J. Am. Chem. Soc.* **2002**, *124*, 8389−8397. (k) Akagi, F.; Matsuo, T.; Kawaguchi, H. *Angew. Chem., Int. Ed.* **2007**, *46*, 8778−8781. (l) Hebden, T. J.; Schrock, R. R.; Takase, M. K.; Muller, P. *Chem. Commun.* **2012**, *48*, 1851−1853.

(20) (a) Fryzuk, M. D.; Love, J. B.; Rettig, S. J.; Young, V. G. *Science* **1997**, *275*, 1445−1447. (b) Pool, J. A.; Lobkovsky, E.; Chirik, P. J. *Nature* **2004**, *427*, 527−530.

(21) Gilbertson, J. D.; Szymczak, N. K.; Tyler, D. R. *J. Am. Chem. Soc.* **2005**, *127*, 10184−10185.

(22) Crossland, J. L.; Tyler, D. R. *Coord. Chem. Rev.* **2010**, *254*, 1883−1894.
(23) (a) Komori, K.; Oshita, H.; Mizobe, Y.; Hidai, M. *J. Am. Chem. Soc.* **1989**, *111*, 1939−1940. (b) Fryzuk, M. D.; MacKay, B. A.; Johnson, S. A.; Patrick, B. O. *Angew. Chem., Int. Ed.* **2002**, *41*, 3709−3712. (c) MacKay, B. A.; Munha, R. F.; Fryzuk, M. D. *J. Am. Chem. Soc.* **2006**, *128*, 9472−9483. (d) Ohki, Y.; Fryzuk, M. D. *Angew. Chem., Int. Ed.* **2007**, *46*, 3180−3183. (e) Fryzuk, M. D. *Acc. Chem. Res.* **2009**, *42*, 127−133. (f) Spencer, L. P.; MacKay, B. A.; Patrick, B. O.; Fryzuk, M. D. *Proc. Natl. Acad. Sci. U. S. A.* **2006**, *103*, 17094−17098. (g) Curley, J. J.; Cook, T. R.; Reece, S. Y.; Müller, P.; Cummins, C. C. *J. Am. Chem. Soc.* **2008**, *130*, 9394−9405. (h) Knobloch, D. J.; Lobkovsky, E.; Chirik, P. J. *Nature Chem.* **2010**, *2*, 30−35. (i) Knobloch, D. J.; Sempronot, S. P.; Lobkovsky, E.; Chirik, P. *J. Am. Chem. Soc.* **2012**, *134*, 3377−3386.
(24) Avenier, P.; Taoufik, M.; Lesage, A.; Solans-Monfort, X.; Baudouin, A.; de Mallmann, A.; Veyre, L.; Basset, J. M.; Eisenstein, O.; Emsley, L.; Quadrelli, E. A. *Science* **2007**, *317*, 1056−1060.
(25) (a) Honkala, K.; Hellman, A.; Remediakis, I. N.; Logadottir, A.; Carlsson, A.; Dahl, S.; Christensen, C. H.; Nørskov, J. K. *Science* **2005**, *307*, 555−558. (b) Mortensen, J. J.; Hansen, L. B.; Hammer, B.; Nørskov, J. K. *J. Catal.* **1999**, *182*, 479−488. (c) Shetty, S.; van Santen, R. A. *Top. Catal.* **2010**, *53*, 969−975.
(26) (a) Schrock, R. R. *Angew. Chem., Int. Ed.* **2008**, *47*, 5512−5522. (b) Le Guennic, B.; Kirchner, B.; Reiher, M. *Chem.—Eur. J.* **2005**, *11*, 7448−7460. (c) Cao, Z.; Zhou, Z.; Wan, H.; Zhang, Q. *Int. J. Quantum Chem.* **2005**, *103*, 344−353. (d) Studt, F.; Tuczek, F. *Angew. Chem., Int. Ed.* **2005**, *44*, 5639−5642. (e) Magistrato, A.; Robertazzi, A.; Carloni, P. *J. Chem. Theory Comput.* **2007**, *3*, 1708−1720. (f) Schenk, S.; Reiher, M. *Inorg. Chem.* **2009**, *48*, 1638−1648. (g) Neese, F. *Angew. Chem., Int. Ed.* **2006**, *45*, 196−199. (h) Vázquez-Lima, H.; Guadarrama, P.; Ramos, E.; Fomine, S. *J. Mol. Catal. A* **2009**, *310*, 75−82. (i) Schenk, S.; Le Guennic, B.; Kirchner, B.; Reiher, M. *Inorg. Chem.* **2008**, *47*, 3634−3650. (j) McNaughton, R. L.; Roemelt, M.; Chin, J. M.; Schrock, R. R.; Neese, F.; Hoffman, B. M. *J. Am. Chem. Soc.* **2010**, *132*, 8645−8656.
(27) (a) Basch, H.; Musaev, D. G.; Morokuma, K.; Fryzuk, M. D.; Love, J. B.; Seidel, W. W.; Albinati, A.; Koetzle, T. F.; Klooster, W. T.; Mason, S. A.; Eckert, J. *J. Am. Chem. Soc.* **1999**, *121*, 523−528. (b) Cui, Q.; Musaev, D. G.; Svensson, M.; Sieber, S.; Morokuma, K. *J. Am. Chem. Soc.* **1995**, *117*, 12366−12367. (c) Studt, F.; Tuczek, F. *J. Comput. Chem.* **2006**, *27*, 1278−1291. (d) Studt, F.; MacKay, B. A.; Fryzuk, M. D.; Tuczek, F. *Dalton Trans.* **2006**, 1137−1140. (e) Christian, G.; Stranger, R.; Yates, B. F.; Cummins, C. C. *Dalton Trans.* **2007**, 1939−1947. (f) Christian, G. J.; Terrett, R. N. L.; Stranger, R.; Cavigliasso, G.; Yates, B. F. *Chem.—Eur. J.* **2009**, *15*, 11373−11383. (g) Christian, G.; Stranger, R.; Yates, B. F. *Chem.—Eur. J.* **2009**, *15*, 646−655. (h) Ariafard, A.; Brookes, N. J.; Stranger, R.; Yates, B. F. *Chem.—Eur. J.* **2008**, *14*, 6119−6124. (i) Bates, V. M. E.; Clentsmith, G. K. B.; Cloke, F. G. N.; Green, J. C.; Jenkin, H. D. L. *Chem. Commun.* **2000**, 927−928. (j) Tanaka, H.; Shiota, Y.; Matsuo, T.; Kawaguchi, H.; Yoshizawa, K. *Inorg. Chem.* **2009**, *48*, 3875−3881. (k) Tanaka, H.; Ohsako, F.; Seino, H.; Mizobe, Y.; Yoshizawa, K. *Inorg. Chem.* **2010**, *49*, 2464−2470. (l) Zhang, X. H.; Butschke, B.; Schwarz, H. *Chem.—Eur. J.* **2010**, *16*, 12564−12569. (m) Baskaran, S.; Sivasankar, C. *Eur. J. Inorg. Chem.* **2010**, 4716−4719. (n) Tanaka, H.; Mori, H.; Seino, H.; Hidai, M.; Mizobe, Y.; Yoshizawa, K. *J. Am. Chem. Soc.* **2008**, *130*, 9037−9047. (o) Roy, D.; Navarro-Vazquez, A.; Schleyer, P. V. R. *J. Am. Chem. Soc.* **2009**, *131*, 13045−13053. (p) Yelle, R. B.; Crossland, J. L.; Szymczak, N. K.; Tyler, D. R. *Inorg. Chem.* **2009**, *48*, 861−871. (q) Askevold, B.; Torres Nieto, J.; Tussupbayev, S.; Herdtweck, E.; Holthausen, M. C.; Schneider, S. *Nature Chem.* **2011**, *3*, 532−537.
(28) Li, J.; Li, S. *Angew. Chem., Int. Ed.* **2008**, *47*, 8040−8043.
(29) For the importance of heterolytic cleavage of dihydrogen, see for instance: (a) Noyori, R.; Kitamura, M. *Angew. Chem., Int. Ed.* **1991**, *30*, 49−69. (b) Noyori, R.; Hashiguchi, S. *Acc. Chem. Res.* **1997**, *30*, 97−102. (c) Noyori, R. *Angew. Chem., Int. Ed.* **2002**, *41*, 2008−2022. (d) Welch, G. C.; Juan, R. R. S.; Masuda, J. D.; Stephan, D. W. *Science* **2006**, *314*, 1124−1126. (e) Samec, J. S. M.; Bäckvall, J. E.; Andersson, P. G.; Brandt, P. *Chem. Soc. Rev.* **2006**, *35*, 237−248. (f) Stephan, D. W. *Dalton Trans.* **2009**, 3129−3136. (g) Stephan, D. W.; Erker, G. *Angew. Chem., Int. Ed.* **2010**, *49*, 46−76. (h) Stephan, D. W. *Chem. Commun.* **2010**, *46*, 8526−8533. (i) Comas-Vives, A.; Ujaque, G.; Lledós, A. *Adv. Inorg. Chem.* **2010**, *62*, 231−260. (j) Gordon, J. C.; Kubas, G. J. *Organometallics* **2010**, *29*, 4682−4701. (k) Juarez, R.; Parker, S. F.; Concepcion, P.; Corma, A.; Garcia, H. *Chem. Sci.* **2010**, *1*, 731−738. (l) Berke, H. *ChemPhysChem* **2010**, *11*, 1837−1849. (m) Dobereiner, G. E.; Nova, A.; Schley, N. D.; Hazari, N.; Miller, S. J.; Eisenstein, O.; Crabtree, R. H. *J. Am. Chem. Soc.* **2011**, *133*, 7547−7562. (n) von der Hoh, A.; Berkessel, A. *ChemCatChem* **2011**, *3*, 861−867. (o) Ito, M.; Ikariya, T. *Chem. Commun.* **2007**, 5134−5142. (p) Abdur-Rashid, K.; Clapham, S. E.; Hadzovic, A.; Harvey, J. N.; Lough, A.; Morris, R. H. *J. Am. Chem. Soc.* **2002**, *124*, 15104−15118. (q) Dobereiner, G. E.; Crabtree, R. H. *Chem. Rev.* **2010**, *110*, 681−703.
(30) Clapham, S. E.; Hadzovic, A.; Morris, R. H. *Coord. Chem. Rev.* **2004**, *248*, 2201−2237.
(31) (a) Thieuleux, C.; Quadrelli, E. A.; Basset, J. M.; Döbler, J.; Sauer, J. *Chem. Commun.* **2004**, 1729−1731. (b) Copéret, C.; Grouiller, A.; Basset, J. M.; Chermette, H. *ChemPhysChem* **2003**, *4*, 608−611. Ustynyuk, L. Y.; Aleshkin, I. A.; Suleimanov, Y. V.; Besedin, D. V.; Ustynyuk, Y. A.; Lunin, V. V. *Russ. J. Phys. Chem. A* **2007**, *81*, 752−758. (c) Besedin, D. V.; Ustynyuk, L. Y.; Ustynyuk, Y. A.; Lunin, V. V. *Mendeleev Commun.* **2002**, 173−175. (d) Ustynyuk, L. Y.; Besedin, D. V.; Lunin, V. V.; Ustynyuk, Y. A. *Russ. J. Phys. Chem.* **2003**, *77*, 1139−1144. (e) Besedin, D. V.; Ustynyuk, L. Y.; Ustynyuk, Y. A.; Lunin, V. V. *Russ. J. Phys. Chem.* **2004**, *78*, 1984−1991. (f) Besedin, D. V.; Ustynyuk, L. Y.; Ustynyuk, Y. A.; Lunin, V. V. *Top. Catal.* **2005**, *32*, 47−60. (g) Mikhailov, M. N.; Bagatur'yants, A. A.; Kustov, L. M. *Russ. Chem. Bull.* **2003**, *52*, 1928−1932. (h) Mikhailov, M. N.; Bagatur'yants, A. A.; Kustov, L. M. *Russ. Chem. Bull.* **2003**, *52*, 30−35. (i) Mikhailov, M. N.; Kustov, L. M. *Russ. Chem. Bull.* **2005**, *54*, 300−311.
(32) (a) Solans-Monfort, X.; Clot, E.; Copéret, C.; Eisenstein, O. *J. Am. Chem. Soc.* **2005**, *127*, 14015−14025. (b) Poater, A.; Solans-Monfort, X.; Clot, E.; Copéret, C.; Eisenstein, O. *J. Am. Chem. Soc.* **2007**, *129*, 8207−8216. (c) Blanc, F.; Basset, J. M.; Copéret, C.; Sinha, A.; Tonzetich, Z. J.; Schrock, R. R.; Solans-Monfort, X.; Clot, E.; Eisenstein, O.; Lesage, A.; Emsley, L. *J. Am. Chem. Soc.* **2008**, *130*, 5886−5900.
(33) Solans-Monfort, X.; Filhol, J. S.; Copéret, C.; Eisenstein, O. *New J. Chem.* **2006**, *30*, 842−850.
(34) Avenier, P.; Solans-Monfort, X.; Veyre, L.; Renili, F.; Basset, J. M.; Eisenstein, O.; Taoufik, M.; Quadrelli, E. A. *Top. Catal.* **2009**, *52*, 1482−1491.
(35) Gouré, E.; Avenier, P.; Solans-Monfort, X.; Veyre, L.; Baudouin, A.; Kaya, Y.; Taoufik, M.; Basset, J. M.; Eisenstein, O.; Quadrelli, E. A. *New J. Chem.* **2011**, *35*, 1011−1019.
(36) Becke, A. D. *J. Chem. Phys.* **1993**, *98*, 5648−5652.
(37) Perdew, J. P.; Wang, Y. *Phys. Rev. B* **1992**, *45*, 13244−13249.
(38) Frisch, M. J.; Trucks, G. W.; Schlegel, H. B.; Scuseria, G. E.; Robb, M. A.; Cheeseman, J. R.; Montgomery, J. A., Jr.; Kudin, K. N.; Burant, J. C.; Millam, J. M.; Iyengar, S. S.; Tomasi, J.; Barone, V.; Mennucci, B.; Cossi, M.; Scalmani, G.; Rega, N.; Petersson, G. A.; Nakatsuji, H.; Hada, M.; Ehara, M.; Toyota, K.; Fukuda, R.; Hasegawa, J.; Ishida, M.; Nakajima, T.; Honda, Y.; Kitao, O.; Nakai, H.; Klene, M.; Li, X.; Knox, J. E.; Hratchian, H. P.; Cross, J. B.; Adamo, C.; Jaramillo, J.; Gomperts, R.; Stratmann, R. E.; Yazyev, O.; Austin, A. J.; Cammi, R.; Pomelli, C.; Ochterski, J. W.; Ayala, P. Y.; Morokuma, K.; Voth, G. A.; Salvador, P.; Dannenberg, J. J.; Zakrzewski, V. G.; Dapprich, S.; Daniels, A. D.; Strain, M. C.; Farkas, O.; Malick, D. K.; Rabuck, A. D.; Raghavachari, K.; Foresman, J. B.; Ortiz, J. V.; Cui, Q.; Baboul, A. G.; Clifford, S.; Cioslowski, J.; Stefanov, B. B.; Liu, G.; Liashenko, A.; Piskorz, P.; Komaromi, I.; Martin, R. L.; Fox, D. J.; Keith, T.; Al-Laham, M. A.; Peng, C. Y.; Nanayakkara, A.; Challacombe, M.; Gill, P. M. W.; Johnson, B.; Chen, W.; Wong, M. W.; Gonzalez, C.; Pople, J. A. *Gaussian 03*, Rev. B.04; Gaussian Inc.: Pittsburgh, PA, 2003.
(39) (a) Höllwarth, A.; Böhme, M.; Dapprich, S.; Ehlers, A. W.; Gobbi, A.; Jonas, V.; Köhler, K. F.; Stegmann, R.; Veldkamp, A.; Frenking, G. *Chem. Phys. Lett.* **1993**, *208*, 237−240. (b) Ehlers, A. W.; Böhme, M.; Dapprich, S.; Gobbi, A.; Höllwarth, A.; Jonas, V.; Köhler, K. F.; Stegmann, R.; Veldkamp, A.; Frenking, G. *Chem. Phys. Lett.* **1993**, *208*, 111−114. (c) Andrae, D.; Häussermann, U.; Dolg, M.; Stoll, H.;

Preuss, H. *Theor. Chim. Acta* **1990**, *77*, 123−141. (d) Bergner, A.; Dolg, M.; Kuchle, W.; Stoll, H.; Preuss, H. *Mol. Phys.* **1993**, *80*, 1431−1441.
(40) Kendall, R. A.; Dunning, T. H.; Harrison, R. J. *J. Chem. Phys.* **1992**, *96*, 6796−6806.
(41) (a) Zhao, Y.; Schultz, N. E.; Truhlar, D. G. *J. Chem. Theory Comput.* **2006**, *2*, 364−382. (b) Zhao, Y.; Truhlar, D. G. *Acc. Chem. Res.* **2008**, *41*, 157−167.
(42) Soignier, S.; Taoufik, M.; Le Roux, E.; Saggio, G.; Dablemont, C.; Baudouin, A.; Lefebvre, F.; de Mallmann, A.; Thivolle-Cazat, J.; Basset, J. M.; Sunley, G.; Maunders, B. M. *Organometallics* **2006**, *25*, 1569−1577.
(43) Lauher, J. W.; Hoffmann, R. *J. Am. Chem. Soc.* **1976**, *98*, 1729−1742.
(44) Klahn, A. H.; Sutton, D. *Organometallics* **1989**, *8*, 198−206. (b) MacLachlan, E. A.; Fryzuk, M. D. *Organometallics* **2006**, *25*, 1530−1543. (c) Fomitchev, D. V.; Bagley, K. A.; Coppens, P. *J. Am. Chem. Soc.* **2000**, *122*, 532−533.
(45) Schaniel, D.; Woike, T.; Delley, B.; Boskovic, C.; Gudel, H. U. *Phys. Chem. Chem. Phys.* **2008**, *10*, 5531−5538.
(46) Ballmann, J.; Munhá, R. F.; Fryzuk, M. D. *Chem. Commun.* **2010**, *46*, 1013−1025.
(47) Holland, P. L. *Dalton Trans.* **2010**, *39*, 5415−5425.
(48) Lee, C. T.; Yang, W. T.; Parr, R. G. *Phys. Rev. B* **1988**, *37*, 785−789.
(49) Mayer, J. M. *Acc. Chem. Res.* **2011**, *44*, 36−46.
(50) Allen, A. D.; Harris, R. O.; Loescher, B. R.; Stevens, J. R.; Whiteley, R. N. *Chem. Rev.* **1973**, *73*, 11−20.